First Hybrid Images from a Combined PET and Field-Cycled MRI System

G. A. Bindseil[1], W. B. Handler[1], T. J. Scholl[1], K. M. Gilbert[2], and B. A. Chronik[1]

[1]Department of Physics and Astronomy, The University of Western Ontario, London, Ontario, Canada, [2]Robarts Research Institute, The University of Western Ontario, London, Ontario, Canada

Introduction

There is substantial interest in combining functional and anatomical imaging modalities into hybrid systems [1]. Efforts to combine PET and MRI must overcome the incompatibility of conventional PET detectors based on photomultiplier tubes (PMT) with magnetic fields. There are a number of approaches to PET and MRI modify PET detectors to make them compatible with conventional MRI [2,3]. A different approach is to use field-cycled MRI (FCMRI) with conventional PMT-based PET. In FCMRI, it is possible to rapidly turn all magnetic fields off enabling the use of PMT-based PET detectors [4,5]. The authors present the first dual modality image acquired on a combined PET and FCMRI system.

Apparatus

An FCMRI system with a 9-cm gap for PET detectors in the center of the scanner was used to generate MR images. The polarizing magnet (0.3 T) produces the initial magnetization of the sample. Then, standard MR imaging is done in the environment of a readout field (94 mT) with high spatial and temporal uniformity. The system has a full set of second-order shims to compensate for the increased inhomogeneity introduced by the PET gap and PET detectors. The geometry of the system is shown in Figure 1. All imaging was done with a low-pass birdcage RF coil tuned to operate at 4 MHz.

The PET system consisted of two detectors taken from a clinical PET system placed 36 cm apart on opposite sides connected to coincidence detection hardware through an RF-shielded feed-through panel. Each PET detector consisted of four PMTs mated to a block of BGO scintillator cut into an array of 8x8 crystals each having a pitch 6.5 x 5.5 x 30 mm^3. The crystal array, cut to various depths, enabled position-determination of detected gamma rays through Anger logic.

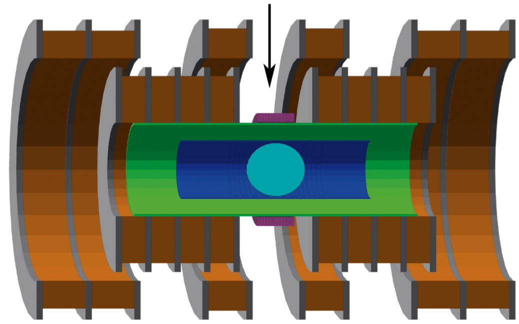

Figure 1. Geometry of PET detectors in field-cycled MRI system. Shown: PET scintillation crystals (purple), gradient coil (green), polarizing magnet (brown, inner), and readout magnet (brown, outer).

Methods

A PET/MR phantom consisting of a triangular arrangement of point sources (Na-22, half-life 2.6 years, total activity 0.11 MBq, 10-mm separation between sources, 1-mm diameter per source, triangular casing with 1-inch side length) embedded in an onion (Figure 3, left) was used to test the feasibility of acquiring a PET and MR image simultaneously. The phantom was placed in the center of the field of view of both systems.

To acquire PET data with two detectors for all lines of response (LOR), it was necessary to rotate the phantom (including RF coil) in 12 steps of 15 degrees and recombine the PET data post-acquisition. For consistency across all phantom rotation angles, PET and MR data were acquired in an interleaved sequence of approximately 0.75 Hz as shown in Figure 2. At each rotation step, a total of 2 minutes of PET data were recorded during a 32 minute MR sequence. The MR image from only the first rotation angle was kept.

The MR imaging parameters were: 3D-FSE; *BW* = 20.03 kHz; *FOV* = 10x10x2 cm; *ETL* = 8; N_{AVG} = 6; Imaging matrix = 192x128x6; *TR/TE* = 2752 ms/21 ms; T_{SCAN} = 32 min; view = single transverse slice. Here, *TR* and T_{SCAN} include PET acquisition stages. PET data were filtered using a 300-700 keV energy window and a 50-ns coincidence-timing window, yielding 120,000 counts. The sinogram was reconstructed using filtered back-projection with no attenuation correction, and two iterations of smoothing (linear interpolation) were applied to the image.

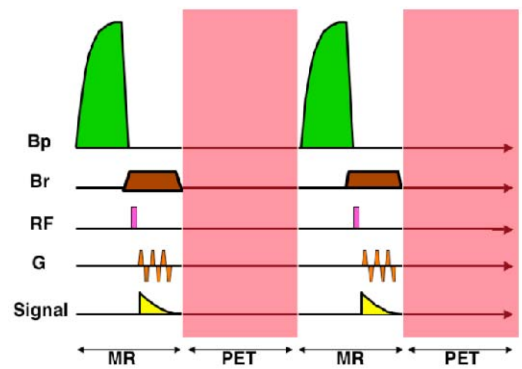

Figure 2. Operational sequence used for interleaved PET/FCMRI system. The duration of MR and PET acquisition stages were ~1.25 s and 1.5 s, respectively.

Results

Figure 3 (right) shows a superposition of PET and MR images acquired in an interleaved manner on the PET/FCMRI system. There are no major streak artifacts in the PET image. There are also no significant phase encoding or ghosting artifacts in the MR image. Since the field-cycled MR system images at low field, there are no apparent susceptibility artifacts due to the presence of the solid radioactive sources.

The resolution of the PET image is limited by the size of the clinical PET detectors, which have coarse position determination compared with modern small-animal PET detectors. Also, the higher reconstructed activity of the lower right point source compared with the others is due to the oversampling of the center of the FOV that occurs when only two detectors are used via a known mechanism. The lower right source was closest to the center of the PET FOV.

Layers of the onion are apparent in the MR image. On the reverse side of the triangular source, a small section of onion protruded into the interior of the triangular hole and is visible in the top left edge of the hole in the MR image.

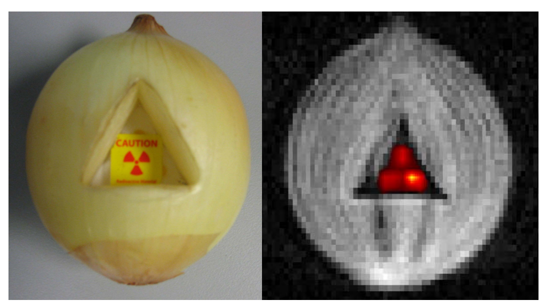

Figure 3. (left) Photograph of phantom, consisting of a triangular arrangement of radioactive point sources inside an onion with a triangular hole cut through its center. **(right)** Superimposed PET (red) and MR (gray) images of the onion phantom. The MR image is a single transverse slice (cropped from original 10 x 10 cm FOV).

Discussion

The successful generation of the first dual modality PET/FCMRI image motivates the authors to pursue the development of an integrated PET/FCMRI system using more appropriate high-performance microPET technology for small-animal imaging with FCMRI at higher fields [6].

[1] Gaa, J., *et al. Eur. J. Med. Res.* (2004) **9**:309-312
[2] Judenhofer M., *et al. Nature Med.* (2008) **14**:459-465
[3] Lucas, J., *et al. IEEE Nuc. Sci. Symp. Conf. Record.* (2006) **4**:2345-2348
[4] Gilbert, K., *et al. Phys. Med. Biol.* (2006) **51**:2825-2841
[5] Handler,W., *et al. Phys. Med. Biol.* (2006) **51**:2479-2491
[6] Bindseil G., *et al. Proc. 16th ISMRM* (2008) p351